BEST AVAILABLE IMAGES

Defective images within this document are accurate representations of the original documents submitted by the applicant.

Defects in the images may include (but are not limited to):

- BLACK BORDERS
- TEXT CUT OFF AT TOP, BOTTOM OR SIDES
- FADED TEXT
- ILLEGIBLE TEXT
- SKEWED/SLANTED IMAGES
- COLORED PHOTOS
- BLACK OR VERY BLACK AND WHITE DARK PHOTOS
- GRAY SCALE DOCUMENTS

IMAGES ARE BEST AVAILABLE COPY.

As rescanning documents *will not* correct images, please do not report the images to the Image Problem Mailbox.

Analysis of changes to song

To characterize changes to the structure of individual syllables, we used a subjective scoring procedure similar to that employed in previous studies of birdsong[16–20]. Observers who were blind to the experimental manipulation of each bird scored the similarity between spectrographic representations of syllables from songs recorded before any manipulation and those from later songs. For each baseline syllable that was initially present in the repertoire of a bird (5–12 distinct syllables per bird), observers identified the most similar syllable present in songs recorded at later dates. Observers additionally judged the degree of similarity between each baseline syllable and its best match on a scale of 0 (no similarity) to 3 (identical). As a measure of the maximum expected deterioration of syllables, we determined the random similarity between syllables of songs from unrelated birds (n = 12 pairs of songs). This random similarity averaged 0.9, indicating some generic similarity between the syllables of unrelated zebra finches. Scores were averaged across 3 observers (mean r^2 for pairwise correlation of observers' scores, 0.81). All songs were recorded from birds isolated in sound attenuating boxes and were therefore 'undirected'. Significance of differences between groups was based on a criterion of $P < 0.05$ using analysis of variance (ANOVA) and post-hoc Fischer's Protected Least Significant Difference tests.

To assess temporal stability, songs were represented by the timing of syllable production, while the spectral structure of individual syllables was ignored. For each bird, the timing pattern representing the most common motif before any experimental manipulation was identified. We then searched songs from later recording sessions for the pattern of syllables that provided the closest temporal match to the initial motif. At each offset (in increments of 5 ms) between motif and song, we quantified the temporal overlap as the average of the percentage overlap of syllables and the percentage overlap of intervals. For each bird, the maximal overlap was calculated for 10 songs and then averaged to provide a measure ('xcorr') of how well the temporal pattern of song was conserved following experimental manipulation. Because the delivery of some songs speeded up 'proportionately' over time (that is, with no apparent change in the relative durations of notes and intervals), we allowed for proportional changes in the temporal pattern of the song (ranging from 75% to 110% of initial song duration) in searching for the maximal overlap. To control partially for varying complexity of different birds' motifs, we calculated the maximal overlaps between each bird's motif and randomly selected songs from unrelated birds ('rand'). The temporal stability of song was then expressed as a normalized value ranging from 0 (indicating no more preservation of temporal pattern than random) to 1 (indicating perfect preservation of temporal pattern). The baseline motif for one pair of brothers had a very simple temporal pattern (3 syllables) and consequently showed a high degree of temporal similarity to all songs (including those from unrelated birds). This pair of birds was therefore excluded from further analysis of changes in temporal pattern.

Received 12 December 1999; accepted 1 February 2000.

1. Nordeen, K. W. & Nordeen, E. J. Auditory feedback is necessary for the maintenance of stereotyped song in adult zebra finches. *Behav. Neural Biol.* **57**, 58–66 (1992).
2. Cowie, R. & Douglas-Cowie, E. *Postlingually Acquired Deafness: Speech Deterioration and the Wider Consequences* 1–304 (Mouton de Gruyter, Berlin, 1992).
3. Marler, P. A comparative approach to vocal learning: song development in white-crowned sparrows. *J. Comp. Physiol. Psychol.* **71**, 1–25 (1970).
4. Doupe, A. J. & Kuhl, P. K. Birdsong and human speech: common themes and mechanisms. *Annu. Rev. Neurosci.* **22**, 567–631 (1999).
5. Leonardo, A. & Konishi, M. Decrystallization of adult birdsong by perturbation of auditory feedback. *Nature* **399**, 466–470 (1999).
6. Houde, J. F. & Jordan, M. I. Sensorimotor adaptation in speech production. *Science* **279**, 1213–1216 (1998).
7. Konishi, M. The role of auditory feedback in the control of vocalization in the white-crowned sparrow. *Z. Tierpsychol.* **22**, 770–783 (1965).
8. Bottjer, S. W. & Johnson, F. Circuits, hormones, and learning: vocal behavior in songbirds. *J. Neurobiol.* **33**, 602–618 (1997).
9. Nottebohm, F., Stokes, T. M. & Leonard, C. M. Central control of song in the canary, *Serinus canarius*. *J. Comp. Neurol.* **165**, 457–486 (1976).
10. Bottjer, S. W., Miesner, E. A. & Arnold, A. P. Forebrain lesions disrupt development but not maintenance of song in passerine birds. *Science* **224**, 901–903 (1984).
11. Sohrabji, F., Nordeen, E. J. & Nordeen, K. W. Selective impairment of song learning following lesions of a forebrain nucleus in the juvenile zebra finch. *Behav. Neural Biol.* **53**, 51–63 (1990).
12. Scharff, C. & Nottebohm, F. A comparative study of the behavioral deficits following lesions of various parts of the zebra finch song system: implications for vocal learning. *J. Neurosci.* **11**, 2896–2913 (1991).
13. Doupe, A. J. Song- and order-selective neurons in the songbird anterior forebrain and their emergence during vocal development. *J. Neurosci.* **17**, 1147–1167 (1997).
14. Solis, M. M. & Doupe, A. J. Contributions of tutor and bird's own song experience to neural selectivity in the songbird anterior forebrain. *J. Neurosci.* **19**, 4559–4584 (1999).
15. Hessler, N. A. & Doupe, A. J. Singing-related neural activity in a dorsal forebrain-basal ganglia circuit of adult zebra finches. *J. Neurosci.* **19**, 10461–10481 (1999).
16. Nordeen, K. W. & Nordeen, E. J. Long-term maintenance of song in adult zebra finches is not affected by lesions of a forebrain region involved in song learning. *Behav. Neural Biol.* **59**, 79–82 (1993).
17. Vu, E. T., Mazurek, M. E. & Kuo, Y. C. Identification of a forebrain motor programming network for the learned song of zebra finches. *J. Neurosci.* **14**, 6924–6934 (1994).
18. Yu, A. C. & Margoliash, D. Temporal hierarchical control of singing in birds. *Science* **273**, 1871–1875 (1996).
19. Vicario, D. S. Contributions of syringeal muscles to respiration and vocalization in the zebra finch. *J. Neurobiol.* **22**, 63–73 (1991).
20. Morrison, R. G. & Nottebohm, F. Role of a telencephalic nucleus in the delayed song learning of socially isolated zebra finches. *J. Neurobiol.* **24**, 1045–1064 (1993).
21. Williams, H. & Mehta, N. Changes in adult zebra finch song require a forebrain nucleus that is not necessary for song production. *J. Neurobiol.* **39**, 14–28 (1999).
22. Johnson, F. & Bottjer, S. W. Afferent influences on cell death and birth during development of a cortical nucleus necessary for learned vocal behavior in zebra finches. *Development* **120**, 13–24 (1994).
23. Akutagawa, E. & Konishi, M. Two separate areas of the brain differentially guide the development of a song control nucleus in the zebra finch. *Proc. Natl Acad. Sci. USA* **91**, 12413–12417 (1994).
24. Kirn, J. R. & Nottebohm, F. Direct evidence for loss and replacement of projection neurons in adult canary brain. *J. Neurosci.* **13**, 1654–1663 (1993).
25. Graybiel, A. M., Aosaki, T., Flaherty, A. W. & Kimura, M. The basal ganglia and adaptive motor control. *Science* **265**, 1826–1831 (1994).
26. Knowlton, B. J., Mangels, J. A. & Squire, L. R. A neostriatal habit learning system in humans. *Science* **273**, 1399–1402 (1996).
27. Nakamura, K., Sakai, K. & Hikosaka, O. Effects of local inactivation of monkey medial frontal cortex in learning of sequential procedures. *J. Neurophys.* **82**, 1063–1068 (1999).
28. Klein, D., Zatorre, R. J., Milner, B., Meyer, E. & Evans, A. C. Left putaminal activation when speaking a second language: evidence from PET. *Neuroreport* **5**, 2295–2297 (1994).
29. Bottjer, S. W., Roselinsky, H. & Tran, N. B. Sex differences in neuropeptide staining of song-control nuclei in zebra finch brains. *Brain Behav. Evol.* **50**, 284–303 (1997).
30. Arnold, A. P. The effects of castration on song development in zebra finches (*Poephila guttata*). *J. Exp. Zool.* **191**, 261–278 (1975).

Acknowledgements

We thank M. Stryker, M. Churchland, T. Troyer and K. T. Moortgat for comments on the manuscript, and A. Arteseros, G. Carrillo and A. Tam for technical assistance. This work was supported by a Burroughs Wellcome Fund fellowship of the Life Sciences Research Foundation (M.S.B.), and by the John Merck Fund, the EJLB Foundation and the National Institutes of Health (A.J.D.).

Correspondence and requests for materials should be addressed to M.S.B. (e-mail: msb@phy.ucsf.edu).

SHATTERPROOF MADS-box genes control seed dispersal in *Arabidopsis*

Sarah J. Liljegren*, Gary S. Ditta*, Yuval Eshed†, Beth Savidge*‡, John L. Bowman† & Martin F. Yanofsky*

* *Section of Cell and Developmental Biology, University of California at San Diego, La Jolla, California 92093-0116, USA*
† *Section of Plant Biology, University of California at Davis, Davis, California 95616, USA*

The fruit, which mediates the maturation and dispersal of seeds, is a complex structure unique to flowering plants. Seed dispersal in plants such as *Arabidopsis* occurs by a process called fruit dehiscence, or pod shatter. Few studies[1–3] have focused on identifying genes that regulate this process, in spite of the agronomic value of controlling seed dispersal in crop plants such as canola[4,5]. Here we show that the closely related *SHATTERPROOF* (*SHP1*) and *SHATTERPROOF2* (*SHP2*) MADS-box genes are required for fruit dehiscence in *Arabidopsis*. Moreover, *SHP1* and *SHP2* are functionally redundant, as neither single mutant displays a novel phenotype. Our studies of *shp1 shp2* fruit, and of plants constitutively expressing *SHP1* and *SHP2*, show that these two genes control dehiscence zone differentiation and promote the lignification of adjacent cells. Our results indicate that further analysis of the molecular events underlying fruit dehiscence may allow genetic manipulation of pod shatter in crop plants.

The MADS-box gene family encodes transcriptional regulators involved in diverse aspects of plant development, and phylogenetic and functional studies show extensive redundancy between family members[6–9]. *SHP1* and *SHP2* (previously known as *AGL1* and *AGL5*) were two strong candidates for functional redundancy, as they share 87% identity at the amino-acid sequence level and show almost identical expression patterns in developing *Arabidopsis* fruit (refs 10–12; and C. Ferrándiz, Y.E., J.L.B. and M.F.Y., unpublished results).

‡ Present address: Calgene, Davis, California 95616, USA.

Arabidopsis is typical of the more than 3,000 species of the Brassicaceae, producing dry dehiscent fruit in which two carpel valves are joined to the replum, a thin structure that separates the valves (Fig. 1)[13–17]. At the valve–replum boundary (valve margin), a narrow band of cells develops into the dehiscence zone[13]. Late in fruit development (stage 18/19), breakdown of the middle lamella between dehiscence zone cells leads to detachment of the valve from the replum, allowing seed dispersal (Fig. 1b)[2,13,18]. Lignification of valve margin cells adjacent to the dehiscence zone and of an internal valve cell layer is proposed to contribute to pod shatter (Fig. 1c)[14]. Within the developing gynoecium, *SHP1* and *SHP2* are expressed in four medial domains which become narrow stripes (stage 9) before the valve margin is distinct (stage 12). This expression pattern at the valve margin is maintained after fertilization, indicating that *SHP1* and *SHP2* may function both to specify the valve margin and to direct dehiscence zone development in the mature fruit.

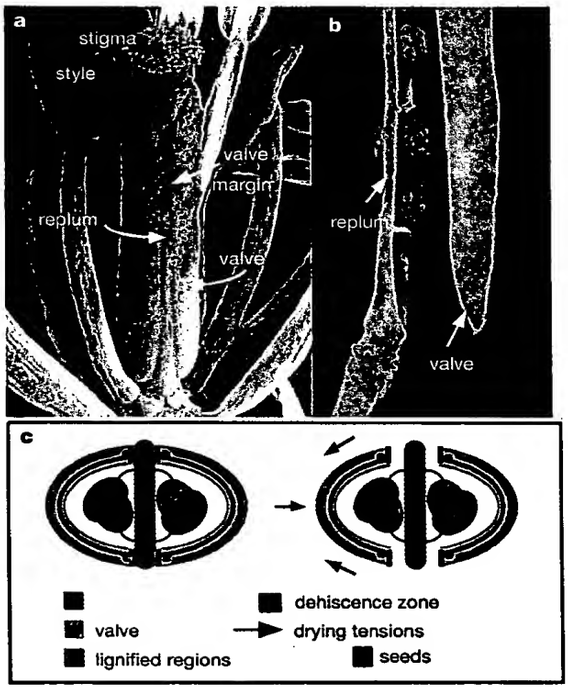

Figure 1 *Arabidopsis* fruit structure and dehiscence. **a**, **b**, Wild-type gynoecium at fertilization (**a**) and during fruit dehiscence (**b**). **c**, Proposed factors contributing to fruit dehiscence. Before dehiscence, small patches of valve margin cells immediately adjacent to the dehiscence zone become lignified, as well as an internal valve cell layer. As the fruit dries, the thin-walled cells of the valves shrink, creating tension within the rigid lignified regions. Once middle lamellar breakdown between dehiscence zone cells occurs, this tension contributes to valve separation from the replum.

Using a polymerase chain reaction (PCR)-based screen of a T-DNA insertional collection, we identified a line containing a disruption in the *SHP1* gene. Subsequent RNA blot analysis confirmed our isolation of a putative *shp1* loss-of-function allele (data not shown). The *SHP2* gene was previously targeted for knockout by homologous recombination[19]. Although both single mutants have putative loss-of-function alleles, *shp1-1* and *shp2-1* fruit show no detectable differences from wild-type fruit (data not shown). In contrast, *shp1 shp2* double mutants have a striking phenotype, as the mature fruit fail to dehisce. Through *shp1* and *shp2* mutagenesis screens for plants producing indehiscent fruit, we have identified additional mutant alleles of *SHP2* and *SHP1*, respectively.

Phenotypic differences between the valve margins of *shp1 shp2* and wild-type fruit are first detected after fertilization. At this point, valve margin cells (about four cell files) in wild-type fruit expand more slowly than valve cells, resulting in a noticeable constriction of the valve margin[13]. Scanning electron microscopy and transverse sections of *shp1 shp2* fruit (stage 14) show less constriction of the valve margins than wild-type fruit (data not shown). Later in wild-type fruit development (stage 16/17), valve margin cells (two cell files) closest to the replum form the dehiscence zone, and separation between dehiscence zone cells begins to occur in mature fruit (stage 18)[13]. Scanning electron microscopy reveals the absence of dehiscence zones in mature *shp1 shp2* fruit at stage 18 (Fig. 2).

As lignification within the fruit may contribute to pod shatter[14], we examined the lignification pattern of *shp1 shp2* fruit using phloroglucinol, a lignin-specific histological stain (Fig. 3). Whereas

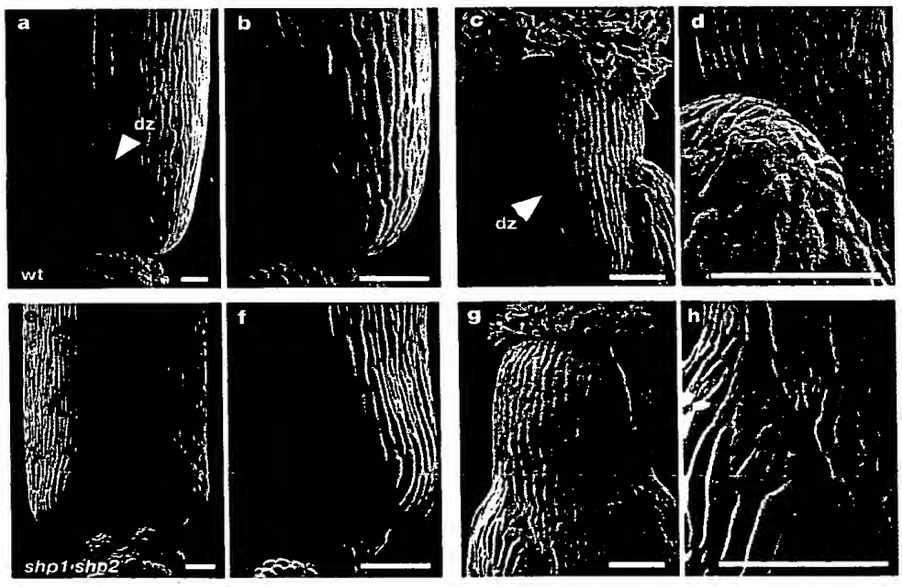

Figure 2 *SHP1* and *SHP2* act redundantly and are required for dehiscence zone differentiation. **a**–**d**, Wild-type (wt) fruit (stage 18) show well developed dehiscence zones (dz) and separation of the valves from the replum is already apparent at the fruit base (**a**, **b**). **e**–**h**, Dehiscence zones are absent in *shp1 shp2* fruit (stage 18). The valve margins of *shp1 shp2* fruit show far less definition than those of wild-type fruit, especially at the fruit base (**e**, **f**). Scale bars, 100 μm.

wild-type fruit (stage 17) show lignification of valve margin cells adjacent to the dehiscence zone throughout the fruit (Fig. 3a, c), we observed a reduction in valve margin cell lignification in *shp1 shp2* fruit. These alterations are regional, as there was no valve margin lignification at the base of *shp1 shp2* fruit (Fig. 3b), but there were lignified valve margin cells toward the fruit apices (Fig. 3d). Lignification of an internal valve cell layer, which occurs slightly later in fruit development[13], is not affected in *shp1 shp2* mutants (Fig. 3b, d).

As our results indicate that *SHP1* and *SHP2* regulate valve margin development, we used two molecular markers derived from gene and enhancer trap screens[20,21] to monitor the cellular differentiation of wild-type and *shp1 shp2* valve margins and to identify possible downstream targets of *SHP1* and *SHP2*. Plants containing the valve margin molecular markers GT140 (ref. 20) and YJ36, which have distinct expression profiles, were crossed to *shp1 shp2* plants. Both markers show very different expression patterns in *shp1 shp2* fruit, demonstrating the altered fate of *shp1 shp2* valve margins (Fig. 4). In wild-type fruit, GT140 is expressed in stripes at the valve margin (Fig. 4a) and in a diffuse domain at the valve base (data not shown). Transverse sections of *shp1 shp2* fruit (stage 17) show that this marker is largely absent from cells at the valve margin (Fig. 4b), although a low level of expression remains at the base of the valves (data not shown). YJ36 is expressed in the outer and inner epidermal cells of the valve margin, the septum and the nectaries of wild-type fruit (Fig. 4c, and data not shown). The valve margin expression domains of this marker are largely absent in *shp1 shp2* fruit whereas the other expression domains remain unchanged (Fig. 4d).

These loss-of-function analyses show that *SHP1* and *SHP2* encode redundant proteins required for proper development of the *Arabidopsis* fruit valve margin, including differentiation of dehiscence zone cells and lignification of valve margin cells adjacent to the dehiscence zone. The altered expression patterns of both GT140 and YJ36 in *shp1 shp2* fruit suggest that their genes act downstream of, and are positively regulated by, *SHP1* and *SHP2*. As these genes are excellent candidates for transcriptional targets of *SHP1* and *SHP2*, we are currently investigating their identity and looking for other downstream targets of *SHP1* and *SHP2* at the valve margin.

No other phenotypes were observed in the *shp1 shp2* double mutant, even though *SHP1* and *SHP2* are also expressed in developing ovules, the septum, the nectaries and the style[11,12]. *SHP1* and *SHP2* activities in these regions may be functionally redundant with other genes, such as the MADS-box genes *AGAMOUS* (*AG*) and *AGL11*, which are closely related to *SHP1* and *SHP2* and are also expressed in developing ovules[22–24]. Further analysis of *SHP1* and *SHP2* function in ovule development may have to await identification of an *agl11* loss-of-function allele and characterization of the *agl11 shp1 shp2* triple mutant.

To complement our loss-of-function analyses of *SHP1* and *SHP2*, we also examined transgenic gain-of-function plants that constitutively express either *SHP1* or *SHP2* under control of the cauliflower mosaic virus 35S promoter[25] (35S::*SHP1* and 35S::*SHP2*). Flowers from plants constitutively expressing *SHP1* or *SHP2* show a phenotype similar to flowers from plants constitutively expressing the MADS-box gene *AG*[26]. Carpelloid sepals and staminoid petals are present in the first and second whorls, respectively, of 35S::*SHP1* and 35S::*SHP2* flowers (data not shown). In addition, 35S::*SHP1* and 35S::*SHP2* fruit show a range of phenotypes, which are most consistent in plants carrying both the *SHP1* and *SHP2* transgenes (Fig. 5). 35S::*SHP1* 35S::*SHP2* fruit are nearly wild-type in length, but have a significantly smaller diameter. The valves of 35S::*SHP1* 35S::*SHP2* fruit (stage 17) have a yellowish-green appearance compared to the dark green colour of wild-type valves, and, before seed maturity, large tears can occur in the valve regions because of seed crowding (Fig. 5a).

Scanning electron microscopy shows that the valves of 35S::*SHP1* 35S::*SHP2* fruit (stage 17) differ from wild-type fruit valves (Fig. 5b). Guard cells and their associated subsidiary cells make up a large fraction of the outer epidermis of wild-type fruit valves (Fig. 2b), but these cells are not apparent in 35S::*SHP1* 35S::*SHP2* valves. Instead, 35S::*SHP1* 35S::*SHP2* valve outer epidermal cells appear homogeneously long and slender. Furthermore, the valve inner epidermis of 35S::*SHP1* 35S::*SHP2* fruit contains about twice as many cells as seen in wild-type fruit (Fig. 5e, f).

Our loss-of-function studies indicate that *SHP1* and *SHP2* promote lignification of a subset of valve margin cells, so we analysed the lignification patterns of fruit that ectopically express

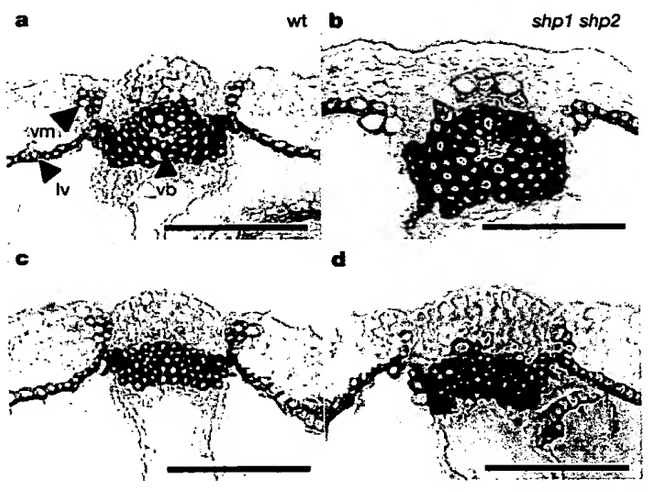

Figure 3 *SHP1* and *SHP2* promote valve margin lignification. Transverse sections of wild-type (**a**, **c**) and *shp1 shp2* (**b**, **d**) fruit (stage 17) were stained with phloroglucinol. Small patches of valve margin (vm) cells immediately adjacent to the dehiscence zones are lignified throughout wild-type fruit (**a**, **c**), whereas these lignified cell patches are not seen at the bases of *shp1 shp2* fruit (**b**) and are reduced elsewhere in *shp1 shp2* fruit (**d**). Lignification of the vascular bundles (vb) or of an internal valve cell layer (lv) is not affected in *shp1 shp2* fruit. Scale bars, 100 μm.

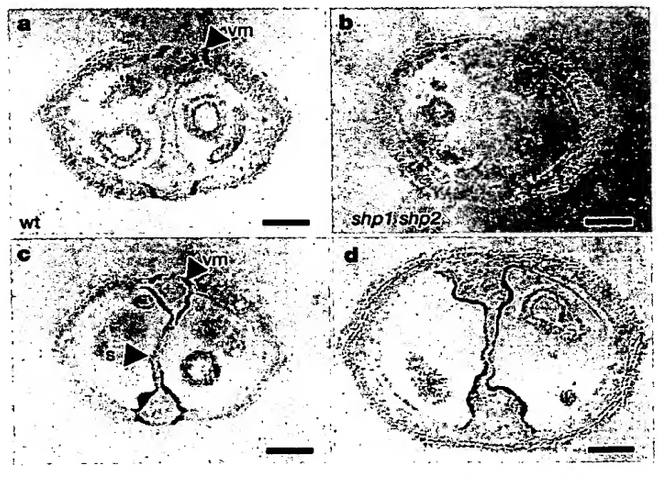

Figure 4 *SHP1* and *SHP2* regulate the expression of valve margin molecular markers. **a**, **b**, In wild-type fruit (**a**), the GT140 marker is expressed in stripes at the valve margin (vm); it is largely absent in *shp1 shp2* fruit (**b**). **c**, **d**, The YJ36 marker is expressed on the outer and inner surfaces of the wild-type valve margin (**c**) but not in *shp1 shp2* (**d**) fruit (stage 17). YJ36 expression is also found within the septum (s) of both wild-type and *shp1 shp2* fruit. Scale bars, 100 μm.

SHP1, *SHP2* or both genes. Although the lignification pattern of 35S::*SHP2* fruit appears identical to that of wild-type fruit, 35S::*SHP1* and 35S::*SHP1* 35S::*SHP2* fruit (stage 17) show ectopic lignification (Fig. 5d, and data not shown) of the valve mesophyll layers, with the most extensive lignification apparent in 35S::*SHP1* 35S::*SHP2* fruit. Cells at positions corresponding to the mesophyll layers are lignified at the valve margins of wild-type fruit (Fig. 5c), so ectopic lignification of the 35S::*SHP1* 35S::*SHP2* valve mesophyll layers suggests that these layers have acquired a lignified valve margin cell identity.

As the GT140 and YJ36 molecular markers demonstrated the altered fate of *shp1 shp2* valve margins, plants containing these markers were crossed to 35S::*SHP1* 35S::*SHP2* plants. GT140 is expressed in stripes at the valve margin of wild-type fruit (Fig. 4a), but in mature 35S::*SHP1* 35S::*SHP2* fruit (stage 16/17) expression of this marker expands throughout the valves (Fig. 5g). Expansion of this marker is consistent with transformation of these valves to a valve margin fate, and with positive regulation of the corresponding gene by *SHP1* and *SHP2*. The expression profiles of YJ36 in wild-type and 35S::*SHP1* 35S::*SHP2* fruit are the same (data not shown), indicating that the corresponding gene is not involved in the transformed valve margin cell identity of 35S::*SHP1* 35S::*SHP2* fruit valves.

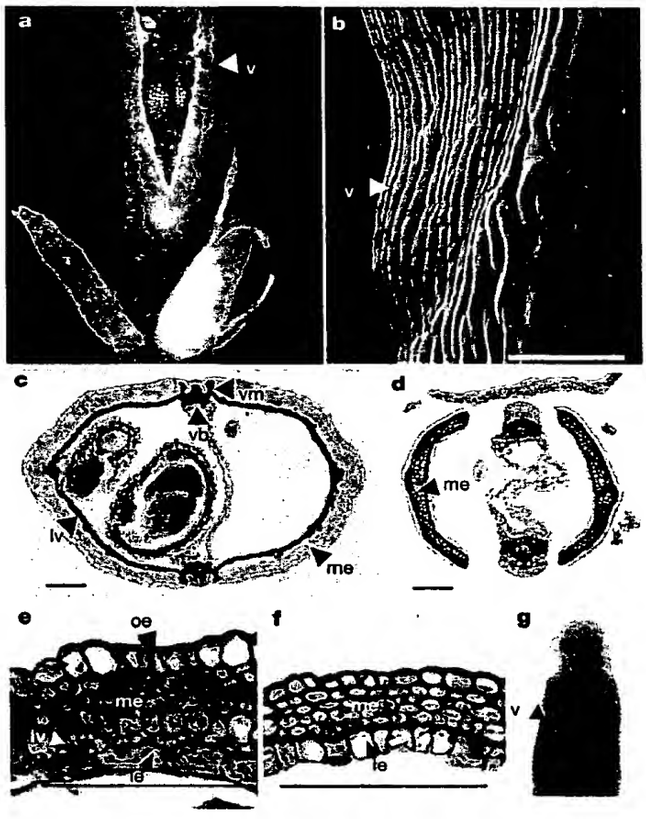

Figure 5 Ectopic expression of *SHP1* and *SHP2* interferes with valve development. **a**, Seed crowding can cause the valves (v) of 35S::*SHP1* 35S::*SHP2* fruit (stage 17) to tear open before fruit dehiscence. **b**, Guard cell differentiation does not occur in the outer epidermis (oe) of 35S::*SHP1* 35S::*SHP2* fruit valves (see wild-type fruit valve, Fig. 2b). Instead, the outer epidermis consists of a homogeneous population of long, slender cells. **c**–**f**, Transverse sections of wild-type (**c**, **e**; stage 17 and 16, respectively) and 35S::*SHP1* 35S::*SHP2* (**d**, **f**) fruit (stage 17) stained with phloroglucinol (**c**, **d**) or toluidine blue (**e**, **f**). The valve mesophyll (me) cell layers are ectopically lignified (**d**) and the valve inner epidermis (ie) has about twice as many cells (**f**) in 35S::*SHP1* 35S::*SHP2* fruit. **g**, Expression of the GT140 valve margin marker expands throughout the valves of 35S::*SHP1* 35S::*SHP2* fruit (stage 16). Scale bars, 100 μm.

These observations indicate that constitutive expression of *SHP1* and *SHP2* throughout the fruit alters development of the valve outer epidermis, the mesophyll layers and the inner epidermis, in a manner consistent with transformation of the valves to a valve margin fate, specifically to that of the valve margin cells adjacent to the dehiscence zone. As valve margin cells do not expand at the same rate as cells throughout the remainder of the valve[13], these transformations may explain the smaller diameter of 35S::*SHP1* 35S::*SHP2* fruit. These gain-of-function analyses suggest that neither *SHP1* nor *SHP2* alone is sufficient to specify a valve margin fate throughout the fruit valve, as the severity of the observed phenotypes is considerably stronger when both transgenes are present. However, it is probable that these two genes do act redundantly and that the severity of the phenotypes is simply a reflection of the higher levels of *SHP* expression in the doubly transgenic plants.

Remarkable phenotypic similarities are apparent between 35S::*SHP1* 35S::*SHP2* fruit and fruit carrying mutant alleles of the *FRUITFULL* (*FUL*) MADS-box gene, although *ful* mutant siliques are much shorter than those of wild-type fruit, and the *ful* mutants exhibit additional phenotypes not seen in 35S::*SHP1* 35S::*SHP2* fruit[27]. In the developing fruit, *FUL* is expressed throughout the valves in a complementary pattern to that of *SHP1/SHP2* at the valve margin, and is required for valve cell differentiation and expansion after fertilization[27,28]. Like 35S::*SHP1* 35S::*SHP2* fruit, *ful* fruit exhibit substantial seed crowding because of a lack of lateral valve expansion, differentiation defects of the valve outer epidermis, ectopic lignification of the valve mesophyll layers and a significantly increased number of valve inner epidermal cells (ref. 27; and S.J.L., C. Ferrándiz and M.F.Y., unpublished results). Similarities also exist between the *shp1 shp2* loss-of-function and 35S::*FUL* gain-of-function phenotypes. Like the *shp1 shp2* double mutants, plants that constitutively express *FUL* also produce indehiscent fruit (C. Ferrándiz, S.J.L. and M.F.Y., unpublished results). These parallels suggest that the *SHP* and *FUL* MADS-box genes may interact antagonistically during valve margin development, and it will be intriguing to explore these possible interactions through expression analyses, construction of the *shp1 shp2 ful* triple mutant and the use of molecular markers.

Arabidopsis is closely related to important oilseed crop plants such as canola (*Brassica napus*, *B. rapa*), where pod shatter causes average annual yield losses of 20% and up to 50% under adverse weather conditions[4,5]. Our studies of *Arabidopsis* fruit dehiscence suggest several molecular strategies to reduce pod shatter in crop plants by genetic engineering. In addition, the availability of *Arabidopsis* mutants that fail to dehisce will allow further investigation of the cascade of gene activity that leads to formation of the valve margin and the programmed series of events within these cells that results in fruit dehiscence. □

Methods

Mutant screens

The *shp1-1* allele was obtained through a PCR-based screen of 5,600 T-DNA insertional lines, using a *SHP1*-specific oligonucleotide (oligo) (5′-CGTTATGAGGGGAAGAAACAA GTTATCATG-3′) and an oligo from the T-DNA left border (5′-GATGCACTCGAAATC AGCCAATTTTAGAC-3′). The T-DNA insertion occurs in the large first intron of the *SHP1* locus. Additional alleles of *SHP1* and *SHP2* were obtained through ethyl methanesulphonate mutagenesis of *shp2-1* and *shp1-1* seed stocks, respectively. More than 4,000 *shp1-1* and 6,000 *shp2-1* M2 families were screened for plants with indehiscent fruit. From these screens, three independent alleles of *SHP2* and four independent alleles of *SHP1* were discovered. The *shp2-2* allele contains a nucleotide substitution at the splice acceptor site of the fourth intron. The same nucleotide substitution at codon 115 in both the *shp1-2* and *shp1-5* alleles changes a glutamine to a stop codon in the K domain, and the *shp1-4* allele contains a nucleotide substitution at the splice donor site of the fourth intron.

Mutant genotyping

Plants homozygous for the *shp1-1* and/or *shp2-1* alleles were identified by PCR genotyping as follows. Amplification with the oligo (5′-GTGACGGAAGGAGGGTTGACG-3′) and a T-DNA specific oligo (above) yields a 597-base pair (bp) product in plants containing the

shp1-1 allele; amplification using the oligos 5′-GTGACGGAAGGAGGGTTGACG-3′ and 5′-GTCTACTGATGAGTTGTCACTAGG-3′ yields an 871-bp product in plants with a wild-type allele of *SHP1*, and no product in plants homozygous for the *shp1-1* allele. Amplification using the oligos 5′-GAGGATAGAGAACACTACGAATCGTC-3′ and 5′-CAGGTCAAGTCAATAGATTCCCTAC-3′ yields a 1.5-kb product in plants with a wild-type allele of *SHP2*, and a single 2.8-kb product in plants homozygous for the *shp2-1* allele.

Generation of transgenic plants

A full-length *SHP1* complementary DNA was created by fusing the *Eco*RI fragments of pCIT2241 and pCIT4219 (ref. 10). The *SHP1* cDNA was then cloned into the *Bam*HI site of pCGN18 (ref. 29), to place *SHP1* transcription under the control of the viral 35S promoter[25]. A full-length *SHP2* cDNA was PCR amplified with the oligos 5′-GGAGATCTGAATTCAT CTTCCCATCC-3′ and 5′-CCGGTACCTCAAACAAGTTG-CAGAGGTGGTTGG TCTTGGTTGGAGGAATTCTGATTCGGTTCAAG-3′, using pCIT2242 (ref. 10) as template. After cloning this product into the TA vector (Invitrogen), a *Bgl*II/*Kpn*I fragment containing the *SHP2* cDNA was cloned into the plant transformation vector pMON530 (Monsanto). The resulting construct also places *SHP2* transcription under control of the 35S promoter. Transgenic plants were selected on kanamycin after *Agrobacterium*-mediated transformation. 35S::*SHP1* plants are in the Landsberg *erecta* ecotype, whereas 35S::*SHP2* plants are in the Columbia ecotype. 35S::*SHP1* and 35S::*SHP2* plants were crossed to each other; in the F1 generation, 35S::*SHP1* 35S::*SHP2* plants were identified by PCR genotyping using *SHP1* transgene-specific (5′-GAAGGTGGGAGTAGTCACGAC-3′ and 5′-CGGAAGGAGGGTTGACGGCA-3′) and *SHP2* transgene-specific (5′-GGTGGTGCGAGTAATGAAGTA-3′ and 5′-TGGTCGGAGGGTTAACGGCG-3′) oligos.

Scanning electron microscopy

Fruit from wild-type (Columbia ecotype), *shp1 shp2* mutants and 35S::*SHP1* 35S::*SHP2* plants were fixed for approximately 4 h at 25 °C in FAA (50% ethanol, 5% glacial acetic acid, 3.7% formaldehyde) and prepared for scanning electron microscopy[27]. Samples were examined in a Cambridge S360 scanning electron microscope using an accelerating voltage of 10 kV.

Histological staining

Tissue from wild-type (Columbia ecotype), *shp1 shp2* and 35S::*SHP1* 35S::*SHP2* plants was fixed, sectioned and stained with toluidine blue[26] with minor modifications. For lignin analyses, sections were stained for 2 min in a 2% phloroglucinol solution in 95% ethanol, then photographed in 50% hydrochloric acid.

Molecular marker analyses

The YJ36 enhancer trap line was generated by *Agrobacterium*-mediated transformation with the plasmid pOCA-28-15-991 (ref. 21). Transgenic plants containing YJ36 or GT140 (ref. 20) were crossed to *shp1 shp2* plants. Among the F2 population, plants with a *shp1 shp2* phenotype that also carried the respective molecular marker were selected for further study. F1 plants from marker crosses to 35S::*SHP1* 35S::*SHP2* plants were genotyped for both transgenes, and analysed further. For β-glucuronidase expression analyses, fruit from GT140, *shp1 shp2* GT140, 35S::*SHP1* 35S::*SHP2* GT140, YJ36, *shp1 shp2* YJ36 and 35S::*SHP1* 35S::*SHP2* YJ36 plants were fixed, sectioned and stained as described[30] with minor modifications.

Received 7 December 1999; accepted 16 February 2000.

1. Jenkins, E. S. *et al.* Characterization of an mRNA encoding a polygalacturonase expressed during pod development in oilseed rape (*Brassica napus* L.). *J. Exp. Bot.* **47**, 111–115 (1996).
2. Petersen, M. *et al.* Isolation and characterisation of a pod dehiscence zone-specific polygalacturonase from *Brassica napus*. *Plant Mol. Biol.* **31**, 517–527 (1996).
3. Coupe, S. A., Taylor, J. E., Isaac, P. G. & Roberts, J. A. Identification and characterization of a proline-rich mRNA that accumulates during pod development in oilseed rape (*Brassica napus* L.). *Plant Mol. Biol.* **23**, 1223–1232 (1993).
4. Child, R. D., Chauvaux, N., John, K., Ulvskov, P. & Onckelen, H. A. Ethylene biosynthesis in oilseed rape pods in relation to pod shatter. *J. Exp. Bot.* **49**, 829–838 (1998).
5. MacLeod, J. in *Oilseed Rape Book* 107–119 (Cambridge Agricultural, Cambridge, 1981).
6. Riechmann, J. L. & Meyerowitz, E. M. MADS domain proteins in plant development. *J. Biol. Chem.* **378**, 1079–1101 (1997).
7. Purugganan, M. D. The MADS-box floral homeotic gene lineages predate the origin of seed plants: phylogenetic and molecular clock estimates. *J. Mol. Evol.* **45**, 392–396 (1997).
8. Bowman, J. L., Alvarez, J., Weigel, D., Meyerowitz, E. M. & Smyth, D. R. Control of flower development in *Arabidopsis thaliana* by *APETALA1* and interacting genes. *Development* **119**, 721–743 (1993).
9. Kempin, S. A., Savidge, B. & Yanofsky, M. F. Molecular basis of the *cauliflower* phenotype in *Arabidopsis*. *Science* **267**, 522–525 (1995).
10. Ma, H., Yanofsky, M. F. & Meyerowitz, E. M. *AGL1-AGL6*, an *Arabidopsis* gene family with similarity to floral homeotic and transcription factor genes. *Genes Dev.* **5**, 484–495 (1991).
11. Flanagan, C. A., Hu, Y. & Ma, H. Specific expression of *AGL1* MADS-box gene suggests regulatory functions in *Arabidopsis* gynoecium and ovule development. *Plant J.* **10**, 343–353 (1996).
12. Savidge, B., Rounsley, S. D. & Yanofsky, M. F. Temporal relationship between the transcription of two *Arabidopsis* MADS box genes and the floral organ identity genes. *Plant Cell* **7**, 721–733 (1995).
13. Spence, J. *Development of the Silique of* Arabidopsis thaliana. Thesis, Univ. Durham (1992).
14. Spence, J., Verchet, Y., Gates, P. & Harris, N. 'Pod shatter' in *Arabidopsis thaliana*, *Brassica napus* and *B. juncea*. *J. Microsc.* **181**, 195–203 (1996).
15. Bowman, J. L., Baum, S. F., Eshed, Y., Putterill, J. & Alvarez, J. Molecular genetics of gynoecium development in *Arabidopsis*. *Curr. Top. Dev. Biol.* **45**, 155–205 (1999).
16. Ferrándiz, C., Pelaz, S. & Yanofsky, M. Control of carpel and fruit development in Arabidopsis. *Annu. Rev. Biochem.* **68**, 321–354 (1999).
17. Rollins, R. C. *The Cruciferae of Continental North America—Systematics of the Mustard Family from the Arctic to Panama* (Stanford Univ. Press, Stanford, 1993).
18. Meakin, P. & Roberts, J. Dehiscence of fruit in oilseed rape (*Brassica napus* L.) I. Anatomy of pod dehiscence. *J. Exp. Bot.* **41**, 995–1002 (1990).
19. Kempin, S. A. *et al.* Targeted disruption in *Arabidopsis*. *Nature* **389**, 802–803 (1997).
20. Sundaresan, V. *et al.* Patterns of gene action in plant development revealed by enhancer trap and gene trap transposable elements. *Genes Dev.* **9**, 1797–1810 (1995).
21. Eshed, Y., Baum, S. F. & Bowman, J. L. Distinct mechanisms promote polarity establishment in carpels of *Arabidopsis*. *Cell* **99**, 199–209 (1999).
22. Yanofsky, M. F. *et al.* The protein encoded by the *Arabidopsis* homeotic gene *agamous* resembles transcription factors. *Nature* **346**, 35–40 (1990).
23. Rounsley, S. D., Ditta, G. S. & Yanofsky, M. F. Diverse roles for MADS box genes in *Arabidopsis* development. *Plant Cell* **7**, 1259–1269 (1995).
24. Bowman, J. L., Drews, G. N. & Meyerowitz, E. M. Expression of the *Arabidopsis* floral homeotic gene *AGAMOUS* is restricted to specific cell types late in flower development. *Plant Cell* **3**, 749–758 (1991).
25. Benfey, P. N. & Chua, N.-H. The cauliflower mosaic virus 35S promoter: combinatorial regulation of transcription in plants. *Science* **250**, 959–966 (1990).
26. Mizukami, Y. & Ma, H. Ectopic expression of the floral homeotic gene *AGAMOUS* in transgenic *Arabidopsis* plants alters floral organ identity. *Cell* **71**, 119–131 (1992).
27. Gu, Q., Ferrándiz, C., Yanofsky, M. & Martienssen, R. The *FRUITFULL* MADS-box gene mediates cell differentiation during *Arabidopsis* fruit development. *Development* **125**, 1509–1517 (1998).
28. Mandel, A. M. & Yanofsky, M. F. The *Arabidopsis AGL8* MADS-box gene is expressed in inflorescence meristems and is negatively regulated by *APETALA1*. *Plant Cell* **7**, 1763–1771 (1995).
29. Jack, T., Fox, G. L. & Meyerowitz, E. M. *Arabidopsis* homeotic gene *APETALA3* ectopic expression: transcriptional and post-transcriptional regulation determine floral organ identity. *Cell* **76**, 703–716 (1994).
30. Blázquez, M. A., Soowal, L. N., Lee, I. & Weigel, D. *LEAFY* expression and flower initiation in *Arabidopsis*. *Development* **124**, 3835–3844 (1997).

Acknowledgements

We thank C. Ferrándiz, A. Sessions, S. Kempin, A. Pinyopich, E. Alvarez-Buylla, J. Spence and N. Harris for helpful discussions; K. Feldmann and his lab for the gift of DNA and seeds from his T-DNA insertional collection; R. Martienssen for providing GT140 seed; and S. Guimil, T. Khammungkhune, C. Chien, H. Cartwright and A. Roeder for assistance with the *shp1* and *shp2* mutagenesis screens. This work was supported by grants from the National Science Foundation, the National Institutes of Health, Monsanto Company and the University of California BioSTAR programme.

Correspondence and requests for materials should be addressed to M.Y. (e-mail: marty@ucsd.edu).

Rapid degradation of a large fraction of newly synthesized proteins by proteasomes

Ulrich Schubert*†, Luis C. Antón*, James Gibbs*, Christopher C. Norbury*, Jonathan W. Yewdell* & Jack R. Bennink*

* *Laboratory of Viral Diseases, National Institute of Allergy and Infectious Diseases, Bethesda, Maryland, USA*
† *Heinrich-Pette Institute, University of Hamburg, Hamburg, Germany*

MHC class I molecules function to present peptides eight to ten residues long to the immune system. These peptides originate primarily from a cytosolic pool of proteins through the actions of proteasomes[1], and are transported into the endoplasmic reticulum, where they assemble with nascent class I molecules[2]. Most peptides are generated from proteins that are apparently metabolically stable. To explain this, we previously proposed that peptides arise from proteasomal degradation of defective ribosomal products (DRiPs). DRiPs are polypeptides that never attain native structure owing to errors in translation or post-translational processes necessary for proper protein folding[3]. Here we show, first, that DRiPs constitute upwards of 30% of newly synthesized proteins as determined in a variety of cell types; second, that at least some DRiPs represent ubiquitinated proteins; and last, that ubiquitinated DRiPs are formed from human immunodeficiency virus Gag polyprotein, a long-lived viral protein that serves as a source of antigenic peptides.